

Direct control of somatic stem cell proliferation factors by the *Drosophila* testis stem cell niche

Eugene A. Albert^{1#}, Olga A. Puretskaia^{1#}, Nadezhda V. Terekhanova^{2,3,4}, Anastasia Labudina¹, Christian Bökel^{1*§}

¹Centre for Regenerative Therapies Dresden, Technical University Dresden, Fetscherstr. 105, 01307 Dresden, Germany

² Sector for Molecular Evolution, Institute for Information Transmission Problems of the RAS (Kharkevich Institute), Moscow 127994, Russia

³N. K. Koltsov Institute of Developmental Biology of the RAS, Moscow 119334, Russia

⁴Laboratory of Molecular Genetics, Russian Federal Research Institute of Fisheries and Oceanography, Moscow 107140, Russia

*current address Department of Biology, Philipps-Universität Marburg, Karl-von-Frisch-Straße 8, 35043 Marburg, Germany

§please address correspondence to christian.boekel@biologie.uni-marburg.de

These authors contributed equally to this work

Summary statement

We demonstrate that the fly testis niche controls directly regulates expression of stem cell proliferation associated genes independent of a binary cell fate decision between stemness and proliferation.

Keywords

DamID / Kibra / Salvador / stem cell niche / Zfh1

Abstract

Niches have traditionally been characterized as signalling microenvironments that allow stem cells to maintain their fate. This definition implicitly assumes that the various niche signals are integrated towards a binary fate decision between stemness and differentiation. However, observations in multiple systems have demonstrated that stem cell properties such as proliferation and self renewal can be uncoupled at the level of niche signalling input, which is incompatible with this simplified view. We have studied the role of the transcriptional regulator Zfh1, a shared target of the Hedgehog and Jak/Stat niche signalling pathways, in the somatic stem cells of the *Drosophila* testis. We found that Zfh1 binds and downregulates *salvador* and *kibra*, two tumour suppressor genes of the Hippo/Wts/Yki pathway, thereby restricting Yki activation and proliferation to the Zfh1 positive stem cells. These observations provide an unbroken link from niche signal input to an individual aspect of stem cell behaviour that does not, at any step, involve a fate decision. We discuss the relevance of these findings for an overall concept of stemness and niche function.

Introduction

Stem cell proliferation and maintenance are typically regulated by niches, signalling microenvironments within tissues that allow resident stem cells to fulfill their functions (Scadden, 2014). Since the first niches were characterized at the molecular level in the *Drosophila* ovary (Xie and Spradling, 2000) and testis (Kiger et al., 2001; Tulina and Matunis, 2001), niche-based regulation of stem cells has largely been discussed using a conceptual framework that considers stemness and differentiation as alternative outcomes of a cell fate decision. Niches were accordingly seen as a means by which the organism can influence this binary decision (Fuller and Spradling, 2007). However, this simplified model is at odds with recent observations in various model systems, including again the *Drosophila* gonadal stem cell niches. For example, stem cell proliferation and self-renewal in the fly testis were shown to be genetically separable at the level of Hh niche signalling input (Amoyel et al., 2013; Michel et al., 2012). Similarly, experimentally altering MAPK activity can uncouple stem cell self-renewal from the regulation of stem cell competitiveness (Amoyel et al., 2016a; Singh et al., 2016). These observations raise fundamental questions about the nature of stemness and the function of niches.

The *Drosophila* testis offers an excellent model system to address such issues. At the tip of the testis, two types of stem cells, the germline stem cells (GSCs) and the somatic cyst stem cells (CySCs), surround a group of postmitotic, somatic niche cells termed hub that provides multiple niche signals regulating both stem cell pools (Figure 1A). In the somatic lineage, the CySCs are the only dividing cells, giving rise to differentiating cyst cells (CyCs) that exit the niche with the developing germline clusters (Losick et al., 2011). CySC maintenance and proliferation requires niche signals by Unpaired (Upd) (Leatherman and Dinardo, 2008) and Hedgehog (Hh) (Amoyel et al., 2013; Michel et al., 2012). Both ligands are produced by the hub and activate the Jak/Stat and Smoothened signalling cascades, respectively, within the CySCs. Even though the two pathways each have multiple, specific targets, they converge on the large, zinc finger and homeodomain containing transcription factor Zfh1 (Fortini et al., 1991). Zfh1 marks the somatic CySC pool within the testis and is absent from differentiated CyCs (Leatherman and Dinardo, 2008) (Figure 1B). Similar to clonal inactivation of either Hh or Upd signalling, removal of their shared target *zfh1* leads to the loss of the mutant CySCs from the stem cell pool by

differentiation (Amoyel et al., 2013; Leatherman and Dinardo, 2008; Michel et al., 2012). *Zfh1* is thus required for CySC stemness.

It has been proposed that *Zfh1* expression is also sufficient for CySC proliferation and self-renewal (Leatherman and Dinardo, 2008). However, the evidence for this is less clear: *Upd* overexpression or Jak/Stat pathway overactivation causes the proliferation of *Zfh1* positive, CySC-like cells (Leatherman and Dinardo, 2008) (Figure 1C) that retain some stem cell characteristics such as proliferation (Leatherman and Dinardo, 2008) but also acquire certain niche properties including the expression of BMP ligands (Leatherman and Dinardo, 2010). This renders them able to recruit GSCs, a niche activity endogenously restricted to the hub (Inaba et al., 2015; Kawase et al., 2004; Michel et al., 2011), resulting in proliferating mixed lineage tumours. Prolonged overexpression of *Zfh1* indeed causes a similar phenotype. However, while increased CySC proliferation in response to *Zfh1* overexpression is rapidly detectable, tumour formation only becomes observable after weeks of overexpression (Leatherman and Dinardo, 2008), suggesting that additional regulatory events or signalling inputs must be involved.

Furthermore, overactivation of the Hh pathway also upregulates *Zfh1* expression and causes accelerated proliferation of the mutant clones (Amoyel et al., 2013; Michel et al., 2012). However, despite initially expressing high levels of *Zfh1*, the affected cells retain the ability and propensity to differentiate (Amoyel et al., 2013; Michel et al., 2012), again suggesting that *Zfh1* expression alone is insufficient for CySC fate.

We therefore hypothesized that a core role of *Zfh1* was to promote CySC proliferation in response to either niche signal, and decided to identify *Zfh1* target genes by mapping its binding sites in the CySCs through an *in vivo* DamID approach (Southall et al., 2013).

Here we report that i) *Zfh1* binds to the putative control regions of multiple genes encoding upstream components of the Hippo/Warts/Yki signalling cascade, including the tumour suppressors *sav* and *kibra*, that ii) *Zfh1 in vivo* partially suppresses the transcription of these two genes, and that iii) activation of Yki, which is necessary and sufficient for stem cell proliferation, is endogenously restricted to the *Zfh1* positive CySCs.

Niche signal input can thus directly be linked with transcriptional regulation of proliferation associated genes, and none of the intervening steps constitutes a cell fate decision establishing stemness. We discuss the implications of these and other recent results for the overall concept of stemness, and propose an alternative model of niche function, whereby multiple niche signals directly and independently "micromanage" distinct subsets of stem cell behaviour.

Results

C-terminally tagged Zfh1 fusion proteins are functional

Visualization of expression patterns by GFP reporters and temporally and spatially controlled expression using the Gal4 system are key elements of the *Drosophila* toolbox. The *zfh1* locus possesses two transcription starts separated by about 17kb. The respective transcripts are spliced to common 3' exons (Figure 1D), giving rise to two isoforms that are both expressed in the testis (Figure S1). *zfh1-RA* encodes a 747aa protein containing seven C2H2 zinc fingers and a central homeodomain, while the 1045aa protein encoded by *zfh1-RB* contains two additional, N-terminal zinc fingers and a polyQ region. We therefore targeted GFP to the common C-terminus of both isoforms (Figure 1D) by Crispr/Cas9-mediated recombination (Gratz et al., 2014; Port et al., 2014). The resulting *zfh1::GFP* knockin lines were homozygous viable and fertile. *Zfh1::GFP* marks the nuclei of somatic cells in the vicinity of the hub (32.7 ± 4.2 GFP⁺ cells/testis, n=20 testes), coinciding with the expression of endogenous *Zfh1* ($94.3 \pm 7.3\%$ GFP and anti-*Zfh1* double positive, n=20) (Figure 1E).

To generate a driver line that captures expression of both isoforms we fused Gal4 to the *Zfh1* C-terminus via a cotranslationally separating T2A peptide (Szymczak et al., 2004) (Figure 1D). The *zfh1::T2A::Gal4* knockin flies were subviable in the homozygous state (ca. 60% of expected adults hatching) and largely male sterile over a deficiency deleting the *zfh1* locus. Viability improved to Mendelian ratios and fertility recovered when the *w*⁺ transgenesis marker was excised. In the larva, *zfh1::T2A::Gal4* driven expression of nls-RFP encompassed multiple tissues with known *Zfh1* presence (Broihier et al., 1998; Lai et al., 1991), including e.g. musculature, heart, nervous system, hemocytes, and gonads (Figure 1F). In the adult

testis, RFP expression under control of *zfh1::T2A::Gal4* was confined to the endogenously *Zfh1* positive CySCs (Figure 1G), demonstrating that the knockin line can direct transgene expression to our cells of interest.

Zfh-1 can therefore in principle tolerate C-terminal fusions. Since the existing UAS constructs (Postigo and Dean, 1999) are based on *zfh1-RB*, we opted for C-terminal modification of this isoform for the cDNA based DamID constructs described below.

***Zfh1* binding sites identified by DamID in S2 cells are enriched at active regulatory regions**

To identify *Zfh1* target sites in the genome we chose a NGS based DamID approach based on the TaDa system (Southall et al., 2013) that uses an mCherry leader ORF (LT3) to achieve the desired, low expression levels of the Dam and Dam fusion proteins (Figure S2A). We first validated this approach for *Zfh1* in S2 cells that also endogenously express *Zfh1* (Figure S2B). We generated stably transfected, polyclonal S2 cell lines expressing either LT3-Dam or LT3-*Zfh1::Dam* under control of the metallothionein promoter. Applying the `damid_seq` analysis pipeline (Marshall and Brand, 2015) to our samples flagged 1125 peaks (Figure 2A, supplementary Table S1) associated with 1052 genes (association criterium distance between DamID peak and ORF < 1kb) based on two replica experiments (Pearson's product-moment correlation between replicates $r = 0.91$ (Dam) and $r = 0.86$ (*Zfh1::Dam*)) (Figure 2B, supplementary Table S1). Using a resampling / permutation approach (Zhu et al., 2010) we found that the S2 *Zfh1* DamID peaks exhibited significant overlap with *Zfh1* binding sites previously identified by ChIPseq in Kc167 cells (Negre et al., 2011) ($n=134$, permutation test, $p<0.001$). To visualize the significance of these observations, the experimentally observed number of overlaps was plotted together with the distribution of overlaps resulting from the randomized resampling (Figure 2C). Significant overlap was also observed between the genes associated with the *Zfh1* peaks in either cell type ($n=179$, χ^2 -test, $p<0.0001$) (Figure 2D). In addition, 70% of the *Zfh1* DamID peaks we identified in S2 cells coincided with regions flagged as enhancers in the same cell type by STARR-seq (Arnold et al., 2013) (Figure S2C), again significantly more than expected by chance ($n=785$, permutation test, $p<0.001$) (Figure 2E).

Finally, we assayed whether the genes associated with the Zfh1 DamID peaks were under Zfh1 transcriptional control. For this, we analysed the transcriptome of S2 cells overexpressing a Zfh1 version unable to bind the transcriptional corepressor CtBP (Zfh1-CIDm) (Postigo and Dean, 1999). Since Zfh1-CIDm is not a full dominant negative but is expected to inactivate only one of several modes of transcriptional regulation by Zfh1, as shown for its mammalian homologue ZEB1 (Gheldof et al., 2012), cells similarly overexpressing WT Zfh1 were chosen as the most closely matched control sample. Upon overexpression of Zfh1-CIDm, 230 out of all 1052 genes associated with Zfh1 DamID peaks (21.9%) exhibited the expected signature of transcriptional derepression (Figure 2F,G). A comparable number instead showed decreased transcription levels relative to Zfh1 WT control (161/1052; 15.3%) (Figures 2G and S2D), while the majority of genes associated with a Zfh1 peak experienced no significant difference between the two samples (661/1052 genes; 62.8%) (Figures 2G and S2E, supplementary Table S2). Importantly, the fraction of genes exhibiting differences in transcription between samples regardless of direction was significantly higher amongst genes associated with at least one Zfh1 peak than for the overall transcriptome (37.5% vs. 9.3%, χ^2 -test: $p < 0.0001$) (Figure 2H). Thus, the Zfh1 DamID peaks were enriched for Zfh1-dependent regulatory elements.

Identifying Zfh1 target genes *in vivo*

However, there was no way of predicting *a priori* which of the targets identified in cell culture may be relevant *in vivo*. We therefore decided to also map Zfh1 binding sites directly in the CySCs of the adult testis, and generated transgenic flies expressing Zfh1-Dam with the LT3 mCherry leader ORF under UAS control (UAS-LT3-zfh1::Dam) (Figure S3A). To suppress transgene expression prior to induction we recombined tub-Gal80^{ts} transgenes both onto the chromosomes carrying the UAS-LT3-dam or UAS-LT3-zfh1::Dam insertions and onto the zfh1::T2A::Gal4 driver line. Following a 24h pulse of transgene expression DNA was then extracted from dissected testes.

Applying the same analysis as above uncovered 811 Zfh1 peaks (Figure 3A, supplementary Table S3) present in both replicates (Pearson's product-moment correlation between replicates $r = 0.91$ (Dam) and $r = 0.86$ (Zfh1::Dam)), which already in a first pass inspection included potential Zfh1 targets such as *eya* or *shg* (Le Bras and Van Doren, 2006; Leatherman and Dinardo, 2008) (Figure 3B). 377 of these

sites (46%) were also occupied in S2 cells (Figure 3C), corresponding to 420 of the 968 genes associated with *Zfh1* in CySCS (43%) (Figure 3D, supplementary Table S3) 18% of the CySC *zfh1* DamID peaks, again significantly more than expected by chance ($n=150$, permutation test, $p<0.001$), coincided with enhancers identified by STARR-seq in cultured ovarian somatic cells (OSCs) (Arnold et al., 2013), mesodermal cells developmentally related to the CySCs (Figure 3E,F). Significant overlap was also observed between the CySC *Zfh1* DamID peaks and the Kc167 *Zfh1* ChIP peaks ($n=67$, permutation test, $p<0.001$) and between the associated genes ($n=113$, χ^2 -test, $p<0.001$) (Figure S3B,C). Finally, Gene Ontology analysis using Panther GO-Slim (Mi et al., 2016) revealed that a limited number of biological processes (7 of 222 terms) was overrepresented among the putative *Zfh1* target genes (Figures 3G and S3D), amongst which the GO term "signal transduction" immediately raised our interest as a potential link to CySC proliferation.

***Zfh1* binds at or near genes encoding members of the Hippo signalling cascade**

We were therefore intrigued by a cluster of hits in or near genes encoding components of the Hippo signalling cascade. This pathway is associated with cell growth, proliferation, and survival (Enderle and McNeill, 2013; Irvine and Harvey, 2015; Meng et al., 2016), and is necessary and sufficient for CySC proliferation (Amoyel et al., 2014). However, it remained unknown whether or how its activity was regulated by niche signals.

The Hippo signalling cascade consists of a core of two serine/threonine kinases, Hippo (Hpo) and Warts (Wts), that phosphorylates and thus inactivates the effector transcription factor Yki with the help of the associated adaptor proteins Salvador (Sav) (Tapon et al., 2002) and Mob-as-tumour-suppressor (Mats), and scaffolding proteins such as Expanded, Kibra (Baumgartner et al., 2010; Genevet et al., 2010; Yu et al., 2010), and Merlin that recruit the complex to the plasma membrane. Inactivation of the upstream components or the kinase complex by physiological signals or by mutation allows Yki to promote target gene expression. In CySCs, we detected *Zfh1* binding at or near the *kibra*, *sav*, and *mats* genes (Figures 3A and S4). In S2 cells binding was additionally observed near *ex*, *pez*, *wts*, and *sd* but not near *mats* (Figure S4).

The ability of overexpressed Zfh1 to induce CySC proliferation depends on its function as CtBP-dependent transcriptional repressor (Leatherman and Dinardo, 2008; Postigo and Dean, 1999). Upd and/or Hh niche signals produced by the hub could thus potentially locally activate Zfh1 expression in adjacent somatic cells, which would in turn repress multiple Hpo pathway components, thereby activating Yki exclusively in the Zfh1 positive stem cells. Consistently, a transcriptional reporter for Yki activity (*diap1*-GFP4.3), in which a minimal Yki response element from the *diap1* gene drives expression of a nuclear GFP (Zhang et al., 2008), is in the adult testis restricted to the Zfh1 positive CySCs (89±9% of all Zfh1 positive cells and 84±7% *diap*-GFP positive cells double positive) (Figure 4A). Moreover, Zfh1 overexpression in the somatic lineage using the *traffic jam* (Tj)-Gal4 driver expanded the region exhibiting Yki activation (Figure 4B,C), while the associated increase in somatic cell count was sensitive to *yki* copy number (Figure S5A,B).

For the remaining experiments we focused on two of the putative target Zfh1 genes, *sav* and *kibra*.

Sav and Kibra limit CySC proliferation

We first confirmed that *kibra* and *sav* affected proliferation in the testis, as previously shown for *hpo* (Amoyel et al., 2014). Homozygous *kibra* clones rapidly expanded relative to controls (Figure 4D,E). BrdU labelling confirmed that this was caused by increased proliferation (Figure S5C,D). Homozygosity for *kibra* did not block differentiation, as indicated by the expression of both the CySC marker Zfh1 and the CyC differentiation marker Eya (Fabrizio et al., 2003) in different mutant cells within the same testis (Figure 4F). Consequently, both three and five days after clone induction (ACI) the fraction of Zfh1 positive cells did not differ between control and *kibra* mutant clones (Figure 4G). The increased proliferation of the *kibra* mutant cells is thus uncoupled from their ability and propensity to differentiate.

The effect of clonal inactivation of *sav* was less pronounced in the short term but was, as for *kibra*, readily detectable by increased long term retention of the clones, reflecting a reduced rate of loss from the niche due to skewed neutral competition (Amoyel et al., 2014) (Figure S5E,F).

Kibra is expressed in the somatic lineage and is downregulated by ectopic Zfh1 expression

We therefore wanted to know whether Kibra expression was reduced in the CySCs under physiological condition. However, in the adult testis, Kibra antibody staining marks most strongly the spectrosomes and fusomes in the germline (Figure 5A), even though the Hpo pathway does not regulate the proliferation of this lineage (Amoyel et al., 2014; Sun et al., 2008). In the soma, Kibra protein could with confidence only be observed in the hub, while the diffuse staining at the interface of germline and somatic cells could not be assigned to either lineage due to their tight apposition.

To assess *kibra* transcription in the testis we therefore generated a construct containing *kibra* exons 5-9, C-terminally fused to a nuclear GFP via a T2A site. This construct was then targeted to a MiMIC landing site (MI13703) (Venken et al., 2011) inserted in the fourth intron of the *kibra* locus (Figure 5B), resulting in viable and fertile *kibra::T2A::GFP* flies. Nuclear GFP expression clearly demonstrated *kibra* expression in both germline and soma. Within the somatic lineage nuclear GFP immunofluorescence was strongest in the hub (184% of median GFP levels in CyCs) (Figure 5C,D). A somewhat weaker signal was also visible in CySCs, identified here as cells abutting the hub and expressing the somatic nuclear marker Tj, and in recently differentiated CyCs (Tj positive cells one tier further out) (Figure 5C). Compared with the CyCs, median nuclear GFP levels in the CySC were reduced by 23% (Figure 5D), consistent with the hypothesis that *Zfh1* downregulates *kibra* transcription.

However, the presence of multiple *Zfh1* DamID peaks near and within the *kibra* transcription unit (Figure S4) made it impractical to test directly whether *kibra* expression in the CySCs is downregulated by endogenous *Zfh1* by deleting the corresponding binding sites. Conversely, clonal inactivation of *Zfh1* causes the rapid exclusion of the mutant cells from the stem cell compartment (Leatherman and Dinardo, 2008), making it impossible to decide whether a possible effect on *kibra* expression were directly caused by the absence of *Zfh1*, or were a consequence of differentiation.

We therefore turned to mosaic expression of *Zfh1* in hub cells, which endogenously express *Kibra* but not *Zfh1*. This allowed us to test *in vivo* whether *Zfh1* expression was sufficient to suppress *kibra* transcription activated by other transcription factors. In line with the observations on the *Zfh1* positive CySCs and their *Zfh1* negative progeny, GFP levels in hub cell nuclei overexpressing *Zfh1* were reduced by 15% relative to their non-overexpressing neighbours (Figure 5E,F).

Sav expression is sensitive to endogenous *Zfh1*

Unlike *kibra*, the *sav* locus possesses only a single *Zfh1* DamID peak located 3' of the coding region (Figure 3A). To test whether endogenous *Zfh1* expression is sufficient for downregulating its target genes we therefore concentrated on *Sav*, using a series of GFP based transcriptional reporter constructs inserted in the attB2 landing site by Φ C31 mediated recombination (Figure 6A).

For this, we isolated a genomic fragment spanning the *sav* genomic region, including parts of the flanking transcription units and the entire *Zfh1* DamID peak. As for *Kibra*, we tagged *Sav* with T2A::GFPnls. Nuclear GFP from this *sav*::T2A::GFPnls reporter was expressed in the germline, with a weaker signal in the somatic CySCs and CyCs but no expression in the hub (Figure 6B). Since derepression of *sav* in the CyCs might negatively affect stem cell maintenance we next deleted the *Sav* coding region and T2A cassette, generating a pure transcriptional reporter line (Figure 6A). The GFP signal of this GFPnls-full_length construct was indistinguishable from that of the *sav*::T2A:GFPnls reporter, confirming that the *sav* coding region does not include essential cis-regulatory regions (Figure 6B,C).

DamID resolution is intrinsically limited by the separation of the GATC target sites, 1063bp in the case of the *sav* *Zfh1* DamID peak. This region contains a short motif with high similarity (10bp of 12bp identical) to the *Zfh1* homeodomain binding site within the *eve* mesodermal enhancer (Su et al., 1999), that resembles the conserved RCSI homeodomain binding motif originally used for cloning *zfh1* (Fortini et al., 1991). (Figure 6A). Sites corresponding to the degenerate RCSI-like sequence CTAATYRRNTT (Su et al., 1999) were indeed significantly enriched in *Zfh1* DamID peaks from both S2 cells and CySCs (S2 cells: PWMenrich raw score 1.377; p=8.06 E-11; CySCs: raw score 1.421; p=1.377 E-07; Stojnic, R. and Diez, D. (2015), PWMEnrich, R package 4.6.0).

We next removed the central third of *sav/CG17119* intergenic region that includes the single RCSI-like sequence motif within the Zfh1 DamID peak (GFPnls- Δ NsiPst). In the final construct, we selectively deleted this putative Zfh1 binding site (GFPnls- Δ RCSI) (Figure 6A).

We then quantified relative GFP fluorescence in CySC and adjacent CyC nuclei for all four reporter lines (Figure 6B-F). For both the *sav::T2A::GFPnls* and the GFP-full length constructs (Figure 6B,C) GFP fluorescence was about 20% lower in the endogenously Zfh1 positive CySCs (again identified by position and Tj immunostaining) than in their differentiating CyC neighbours (Figure 6F). This difference was abolished for both constructs carrying the deletions within the Zfh1 DamID peak (GFPnls- Δ NsiPst and GFPnls- Δ RCSI) (Figure 6D-F), confirming that the RCSI-like motif is the *cis*-acting element responsible for downregulation of *sav* expression in the Zfh1-positive CySCs.

To test whether the observed, partial reduction in both Sav and Kibra levels could together be sufficient for triggering CySC proliferation we quantified the number of Zfh1 positive CySCs in testes of *sav* and *kibra* single or double heterozygous flies vs. controls. (Fig. 6G). However, there were no significant differences in CySC numbers per testis, suggesting that these stem cells either do not proliferate more strongly when the dose of both Kibra and Sav is reduced, or that the overall size of the stem cell pool is regulated also by additional mechanisms. In addition, epistasis experiments between *zfh1* and *yki* were inconclusive: Neither Zfh1 overexpression in *yki* mutant clones (Fig. S5G) nor expression of dominantly active, nonphosphorylatable Yki (YkiS168A) in *zfh1* mutant cells (Fig. S5H) were able to rescue the loss of the respective clones.

Taken together our observations show that the DamID experiments successfully uncovered target genes regulated by Zfh1 in the adult testis, that the regions flagged as Zfh1 binding peaks contain sequence elements conveying Zfh1 sensitivity, and that Zfh1 downregulates transcription of Hippo pathway components, which may contribute to CySC proliferation and is consistent with the pattern of endogenous Yki activation.

Discussion

Stemness and differentiation have long been treated as alternative outcomes of a binary cell fate decision made by a stem cell that would subsequently govern its behaviour (Fuller and Spradling, 2007). However, we and others had previously shown that experimental activation of the Hh pathway upregulates proliferation of somatic CySCs, but does not affect the differentiation propensity of the mutant clones (Amoyel et al., 2013; Michel et al., 2012). In contrast, overexpression of Upd instead drives the proliferation of stem cell like cells that fail to differentiate but also partially acquire hub functions (Leatherman and Dinardo, 2008). Activation of MAPK signalling can uncouple stem cell self-renewal from the regulation of cell competition and adhesion to the niche (Amoyel et al., 2016a; Singh et al., 2016). Manipulation of either of these endogenously active signalling pathways thus impinges on overlapping but distinct subsets of stem cell properties. However, such partial alteration of stem cell behaviour should not be possible if niche signals became integrated into a decision between stemness and differentiation (Figure 7A).

The results presented here provide a regulatory link between niche signal input and the transcription of genes involved in stem cell proliferation that does not involve any individual step that would be by itself sufficient for stemness: The Hh and Upd niche signals converge on *Zfh1* (Amoyel et al., 2013; Leatherman and Dinardo, 2008; Michel et al., 2012), which we found to bind to multiple genes encoding regulators of the Hippo signalling cascade. For two of these genes, *sav* and *kibra*, we could show that this results in a partial suppression of transcription, as reflected by reduced reporter gene expression in endogenously *Zfh1* positive CySCs. For *sav* we were able to identify a short, putative homeodomain binding motif within the *Zfh1* DamID peak as the *cis*-acting sequence that is necessary to convey repression in endogenously *Zfh1* positive cells. Conversely, *Zfh1* misexpression in the hub demonstrated that *Zfh1* is *in vivo* sufficient to suppress *kibra* transcription driven by other, as yet unknown transcriptional regulators. Even though both genes are downregulated in CySCs by no more than 25%, *Yki* activation in the testis is tightly restricted to the *Zfh1* positive stem cells. Since the loss of one copy of any individual Hpo pathway gene, or even double heterozygosity for *kibra* and *sav*, has no obvious proliferative phenotype we postulate that *Yki* activity is controlled cooperatively through the modulation of multiple regulators that may, in addition, be influenced by multiple

upstream stimuli: While *kibra* and *sav* appear to be transcriptionally controlled by niche signalling via *Zfh1*, the upstream Hippo pathway regulator Merlin has recently been implicated in regulating CySC proliferation in response to cell adhesion (Inaba et al., 2017). Surprisingly, in the ovary Hh regulates Hippo signalling through transcriptional control of *Yki* (Huang and Kalderon, 2014). We currently have no explanation as to why the male and female niches should make use of the same molecular players but follow a different regulatory logic.

Generalizing from this direct link between niche signals and the genes involved in proliferation, and considering other examples where different aspects of stem cell behaviour can be uncoupled at the level of niche signal input (Amoyel et al., 2016a; Leatherman and Dinardo, 2008; Singh et al., 2016), we would like to suggest that the function of the niche is to directly instruct competent cells to execute specific stem cell behaviours. "Stemness" would thus become an operational description given to any cell instructed to self renew and produce differentiating offspring, without having to invoke a cell fate decision. We would like to propose the term "micromanagement" for this mode of niche-mediated stem cell regulation (Figure 7B).

Of course, this model comes with several caveats. First, the somatic CySCs of the fly testis or the stem cells of the mammalian intestinal epithelium (Beumer and Clevers, 2016) may represent one extreme within a continuum of stem cell / niche systems that differ in their relative contributions of fate specification and micromanagement. The mammalian hematopoietic system, which has guided much of our thought about stemness and niches (Scadden, 2014), and indeed the *Drosophila* germline stem cells, which are maintained primarily through suppression of the differentiation factor Bam by a hub derived BMP niche signal (Chen and McKearin, 2003; Kawase et al., 2004) may represent the other end of the spectrum.

Second, the competence of a cell to respond to a given niche microenvironment clearly depends on cell fate decisions along its developmental trajectory: Unlike the CySC/CyC lineage, the muscle sheath of the testis does not respond to Upd or Hh overexpression by proliferating, even though both cell types are of mesodermal origin.

Third, the micromanagement model we propose will still be a truncation of the true regulatory network. For example, we already know that different aspects of stem cell activity in the testis are coupled by competition (Amoyel et al., 2016a; Issigonis et al., 2009; Michel et al., 2012; Singh et al., 2016), making it difficult to analyze loss of function conditions, as affected cells are eliminated by differentiation regardless of the actual function of the affected pathway. In addition, the subsets of stem cell behaviours controlled by different niche signals may overlap, and any individual signal can control multiple aspects of stemness. For example, Upd not only cooperates with Hh to promote CySC proliferation through Zfh1, but independently ensures male specific development of the somatic lineage through Chinmo (Flaherty et al., 2010; Ma et al., 2014).

Interestingly, a corresponding argument may be made for cyst cell differentiation: Recent work from several labs suggests that it, too, appears to be a highly regulated process involving detailed instructions through several niche-like signals, rather than just reflecting a general loss of stemness maintaining factors (Amoyel et al., 2016b; Hudson et al., 2013).

Even Zfh1 itself is likely to control additional aspects of stemness: Hippo pathway components account for only a small fraction of the many hundred potential target genes we identified in the CySCs. We found Zfh1 peaks e.g. also near multiple genes involved in glucose and energy metabolism, with carbohydrate transport appearing as a significantly enriched GO term. This invites the speculation that a potential, Warburg-like stem cell metabolic state (Chandel et al., 2016) may also be the outcome of detailed, continuous regulation by the niche rather than a consequence of stem cell fate. In addition, such additional functions may explain why Yki activation is insufficient to rescue clonal loss of Zfh1.

Finally, under our micromanagement model, the minimal unit of stemness is a stem cell together with its niche. Obviously this can only hold true for tissue resident stem cells that actually are integrated with a niche, but may not apply to embryonic stem cells that are, at least *in vitro*, able to retain their stem cell properties in the absence of a complex signalling microenvironment.

Materials and methods

Fly stocks and transgenic lines

w;UAS-zfh1; w;;UAS-RedStinger; w;;FRT82B w⁺90E; w;Sco/CyO;tub-GAL80^{ts}; y w;MiMIC kibra^{MI13703}; y w;;Act5C>CD2Y>GAL4; and y sc v nos-phiC31Int;;attP2 were obtained from the Bloomington Drosophila Stock Center.

The following stocks were graciously provided by our colleagues: UAS-Hop^{tumL} (Bruce Edgar); y w vasa-Cas9/FM7c (Anne Morbach); UAS-LT3-Dam (Andrea Brand); tj Gal4 Gal80^{ts} (Doug Allan); y w;Sp / CyO, y⁺;FRT82 kibra¹ / TM6B, Tb, Hu; y w;Sp/CyO,y⁺;diap1-GFP4.3/TM6B, Tb; w;FRTD 42D yki^{B5}/CyO (Hugo Stocker); FRT 82B sav³/TM3 Sb (Florence Janody, Nic Tapon).

MARCM clones (Lee and Luo, 1999) were generated by crossing FRT males to w hs-FLP C587-Gal4 UAS-RedStinger virgins carrying the appropriate tub-Gal80 FRT chromosomes and heat shocking adult males for 1h at 37°C.

The zfh1::GFP and zfh1::T2A::Gal4 lines were generated by coinjecting two pU6-BbsI-gRNA plasmids (Gratz et al., 2014) (Addgene 45946) with a pRK2 (Huang et al., 2008) derived plasmid containing the transgene sequence, 1kb homology arms, and a w⁺ selection marker into y w vasa-Cas9/FM7c.

kibra::T2A::GFP was generated by injecting a pBSKS-attB1_2SASD-0 plasmid (Frank Schnorrer) containing kibra exons 5 to 9 fused to T2A-GFPnls into nos-phiC31Int;MiMIC kibra^{MI13703}.

The Sav reporter constructs were generated by fusing a T2A::GFPnls cassette to the Sav C-terminus. The sav coding region and the 3' UTR segments were then excised and deletions introduced to the Zfh1 DamID peak.

For UAS-LT3-zfh1::Dam the zfh1-RB ORF (Korneel Hens) was inserted into pUAST-attB-LT3-Dam (Andrea Brand).

Full sequences are available upon request.

Antibodies and immunohistochemistry

Testes were stained as described (Michel et al., 2011), incorporating an 1h incubation with 1% Triton X-100 following fixation. The following antisera were used: rat-anti-DECadherin (DSHB, DCAD2) 1:100, mouse-anti-Eya (DSHB, eya10H6) 1:20, mouse-anti-FasIII (DSHB, 7G10) 1:100, rabbit-anti-GFP (Clontech) 1:500, rabbit-anti-Kibra (Nic Tapon) 1:200, rat-anti-Tj (Dorothea Godt) 1:250, Rabbit anti-vasa (Paul Lasko) 1:5000, rabbit-anti-Zfh1 (Ruth Lehmann) 1:4000. Alexa-488, -568, or -633 secondary ABs (Invitrogen) were used 1:500.

BrdU labeling

Flies were fed on food containing 2 mg/ml BrdU for 8h. In addition to the regular immunostaining protocol testes were incubated for 30min in 2M HCl, neutralized with 100mM borax solution and incubated with mouse anti-BrdU-Alexa 488 (BD) 1:200 over night.

Imaging and image analysis

Images were acquired using Leica SP5, Zeiss LSM700, and Zeiss LSM780 confocal microscopes with 40x or 63x water immersion objectives. Unless stated otherwise, images are single optical slices. Image quantifications were performed using Fiji (Schindelin et al., 2012), applying a double blind protocol where appropriate. Image quantifications were tested for significance using Student's t-test or ANOVA followed by Tukey's HSD as appropriate. Images were prepared for publication using Adobe Photoshop and Illustrator.

Cell culture

S2 cells were cultivated in Schneider's Drosophila Medium (Pan Biotech) with 10% FBS (Thermo Scientific) and transfected using calcium phosphate. The plasmids pMT-LT3-dam, pMT-LT3-zfh1::Dam (Fig. S2), pMT-Zfh1 and pMT-Zfh1-CIDm were generated by placing expression cassettes under control of the metallothionein promoter of pmtn-HhN (Albert and Bökel, 2017). Sequences are available upon request.

RNAseq

Transgene expression from pMT-Zfh1 and pMT-Zfh1-CIDm was induced with 1mM CuSO₄ for 24h before RNA extraction using Direct-zol (Zymo Research). RNA was sequenced by the CRTD/Biotec NGS facility (Illumina HiSeq2000).

DamID

DNA was extracted from stable S2 cell lines transfected with pMT-LT3-Dam or pMT-LT3-zfh1::Dam without Cu²⁺ induction according to the protocol described in (Vogel et al., 2007) omitting steps required for array hybridization.

DNA was extracted from testes proper as described in (Laktionov et al., 2014). In brief, following 24h induction at 30°C hand dissected testes from 50 zfh1::T2A::Gal4 tub-Gal80^{ts}/UAS-LT3-zfh1::Dam tub-Gal80^{ts} or zfh1::T2A::Gal4 tub-Gal80^{ts}/UAS-LT3-Dam tub-Gal80^{ts} males per replica were dissociated in 700µl lysis buffer (0.1M NaCl, 0.2M Sucrose, 0.1M TrisHCl pH 9.1, 0.05M EDTA, 0.5% SDS) by syringe aspiration, before over night incubation at 56°C with 100µg/ml dispase. Following RNase digest and phenol/chloroform extraction samples were processed according to (Vogel et al., 2007), and sequenced by the CRTD/Biotec NGS facility (Illumina HiSeq2000).

Bioinformatics

NGS DamID reads were mapped to the *Drosophila* genome (dm6) using bowtie2. Peaks were called using damid_seq analysis pipeline v1.4.2 (Marshall and Brand, 2015) and the find_peaks script (Marshall and Brand, 2015) with the false discovery rate (FDR) threshold set to 0.01. Overlap of the Zfh1 DamID peaks with other sequence sets was analyzed using the peakPermTest resampling / permutation approach implemented in the ChIPpeakAnno bioconductor package (Zhu et al., 2010) excluding the ENCODE *Drosophila* blacklist (Celniker et al., 2009). For each comparison, we performed 1000 resampling runs artificially redistributing peaks while conserving their distribution of relative positions to landmarks of the respective, associated genes (transcription starts and end, introns, and coding regions). Overlap between associated genes (defined as genes < 1kb distant from the ends of a Zfh1 DamID peak or other feature) was tested for significance using the χ^2 -test.

Enrichment of the degenerate, RCSI-like motif (CTAATYRRNTT) within Zfh1 DamID peaks was tested using PWMenrich (Stojnic, R. and Diez, D. (2015). PWMenrich, R package).

RNASeq analysis was performed using the DESeq R package (Anders and Huber, 2010). Reads were normalized according to the library complexity. Gene annotation was obtained from ENSEMBL (BDGP6 version) using the biomaRt R package (Smedley et al., 2009). Genes were flagged as significantly changing expression if the corresponding adjusted p-values were below 0.05.

Acknowledgements

We would like to thank the colleagues mentioned individually above and the JEDI community for fly stocks, reagents, and advice, the CRTD NGS sequencing facility for their support, Ilker Deniz for help with immunostainings, and Heiner Grandel, Christian Lange, Nikolay Ninov, and Pavel Tomancak for discussions and critical reading of the manuscript. The project was supported by a CRTD seed grant and Deutsche Forschungsgemeinschaft (DFG) grant BO 3270/4-1 to CB.

Author contributions:

OAP and AL performed fly experiments, EAA performed cell culture, DamID, and RNAseq experiments, EAA and NVT performed bioinformatic analysis. All authors analysed and interpreted the data. CB initiated the project and wrote the manuscript.

Data availability

Tabulated DamID and RNAseq results are presented in the supplementary information. The corresponding raw data files are available at the NCBI Sequence Read Archive (BioProject PRJNA475363).

Conflict of interest

The authors declare no conflict of interest.

References

- Albert, E. A. and Bökel, C.** (2017). A cell based, high throughput assay for quantitative analysis of Hedgehog pathway activation using a Smoothened activation sensor. *Sci Rep* **7**, 14341.
- Amoyel, M., Anderson, J., Suisse, A., Glasner, J. and Bach, E. A.** (2016a). Socs36E Controls Niche Competition by Repressing MAPK Signaling in the Drosophila Testis. *PLoS Genet* **12**, e1005815.
- Amoyel, M., Hillion, K. H., Margolis, S. R. and Bach, E. A.** (2016b). Somatic stem cell differentiation is regulated by PI3K/Tor signaling in response to local cues. *Development* **143**, 3914-3925.
- Amoyel, M., Sanny, J., Burel, M. and Bach, E. A.** (2013). Hedgehog is required for CySC self-renewal but does not contribute to the GSC niche in the Drosophila testis. *Development* **140**, 56-65.
- Amoyel, M., Simons, B. D. and Bach, E. A.** (2014). Neutral competition of stem cells is skewed by proliferative changes downstream of Hh and Hpo. *EMBO J* **33**, 2295-2313.
- Anders, S. and Huber, W.** (2010). Differential expression analysis for sequence count data. *Genome Biol* **11**, R106.
- Arnold, C. D., Gerlach, D., Stelzer, C., Boryn, L. M., Rath, M. and Stark, A.** (2013). Genome-wide quantitative enhancer activity maps identified by STARR-seq. *Science* **339**, 1074-1077.
- Baumgartner, R., Poernbacher, I., Buser, N., Hafen, E. and Stocker, H.** (2010). The WW domain protein Kibra acts upstream of Hippo in Drosophila. *Dev Cell* **18**, 309-316.
- Beumer, J. and Clevers, H.** (2016). Regulation and plasticity of intestinal stem cells during homeostasis and regeneration. *Development* **143**, 3639-3649.
- Broihier, H. T., Moore, L. A., Van Doren, M., Newman, S. and Lehmann, R.** (1998). zfh-1 is required for germ cell migration and gonadal mesoderm development in Drosophila. *Development* **125**, 655-666.
- Celniker, S. E., Dillon, L. A., Gerstein, M. B., Gunsalus, K. C., Henikoff, S., Karpen, G. H., Kellis, M., Lai, E. C., Lieb, J. D., MacAlpine, D. M., et al.** (2009). Unlocking the secrets of the genome. *Nature* **459**, 927-930.
- Chandel, N. S., Jasper, H., Ho, T. T. and Passegue, E.** (2016). Metabolic regulation of stem cell function in tissue homeostasis and organismal ageing. *Nat Cell Biol* **18**, 823-832.
- Chen, D. and McKearin, D.** (2003). Dpp signaling silences bam transcription directly to establish asymmetric divisions of germline stem cells. *Curr Biol* **13**, 1786-1791.
- Enderle, L. and McNeill, H.** (2013). Hippo gains weight: added insights and complexity to pathway control. *Sci Signal* **6**, re7.
- Fabrizio, J. J., Boyle, M. and DiNardo, S.** (2003). A somatic role for eyes absent (eya) and sine oculis (so) in Drosophila spermatocyte development. *Dev Biol* **258**, 117-128.
- Flaherty, M. S., Salis, P., Evans, C. J., Ekas, L. A., Marouf, A., Zavadil, J., Banerjee, U. and Bach, E. A.** (2010). chinmo is a functional effector of the JAK/STAT pathway that regulates eye development, tumor formation, and stem cell self-renewal in Drosophila. *Dev Cell* **18**, 556-568.

- Fortini, M. E., Lai, Z. C. and Rubin, G. M.** (1991). The *Drosophila* *zfh-1* and *zfh-2* genes encode novel proteins containing both zinc-finger and homeodomain motifs. *Mech Dev* **34**, 113-122.
- Fuller, M. T. and Spradling, A. C.** (2007). Male and female *Drosophila* germline stem cells: two versions of immortality. *Science* **316**, 402-404.
- Genevet, A., Wehr, M. C., Brain, R., Thompson, B. J. and Tapon, N.** (2010). Kibra is a regulator of the Salvador/Warts/Hippo signaling network. *Dev Cell* **18**, 300-308.
- Gheldof, A., Hulpiau, P., van Roy, F., De Craene, B. and Berx, G.** (2012). Evolutionary functional analysis and molecular regulation of the ZEB transcription factors. *Cell Mol Life Sci* **69**, 2527-2541.
- Gratz, S. J., Ukken, F. P., Rubinstein, C. D., Thiede, G., Donohue, L. K., Cummings, A. M. and O'Connor-Giles, K. M.** (2014). Highly specific and efficient CRISPR/Cas9-catalyzed homology-directed repair in *Drosophila*. *Genetics* **196**, 961-971.
- Huang, J. and Kalderon, D.** (2014). Coupling of Hedgehog and Hippo pathways promotes stem cell maintenance by stimulating proliferation. *J Cell Biol* **205**, 325-338.
- Huang, J., Zhou, W., Watson, A. M., Jan, Y. N. and Hong, Y.** (2008). Efficient ends-out gene targeting in *Drosophila*. *Genetics* **180**, 703-707.
- Hudson, A. G., Parrott, B. B., Qian, Y. and Schulz, C.** (2013). A temporal signature of epidermal growth factor signaling regulates the differentiation of germline cells in testes of *Drosophila melanogaster*. *PLoS One* **8**, e70678.
- Inaba, M., Buszczak, M. and Yamashita, Y. M.** (2015). Nanotubes mediate niche-stem-cell signalling in the *Drosophila* testis. *Nature* **523**, 329-332.
- Inaba, M., Sorenson, D. R., Kortus, M., Salzmann, V. and Yamashita, Y. M.** (2017). Merlin is required for coordinating proliferation of two stem cell lineages in the *Drosophila* testis. *Sci Rep* **7**, 2502.
- Irvine, K. D. and Harvey, K. F.** (2015). Control of organ growth by patterning and hippo signaling in *Drosophila*. *Cold Spring Harb Perspect Biol* **7**.
- Issigonis, M., Tulina, N., de Cuevas, M., Brawley, C., Sandler, L. and Matunis, E.** (2009). JAK-STAT signal inhibition regulates competition in the *Drosophila* testis stem cell niche. *Science* **326**, 153-156.
- Kawase, E., Wong, M. D., Ding, B. C. and Xie, T.** (2004). Gbb/Bmp signaling is essential for maintaining germline stem cells and for repressing bam transcription in the *Drosophila* testis. *Development* **131**, 1365-1375.
- Kiger, A. A., Jones, D. L., Schulz, C., Rogers, M. B. and Fuller, M. T.** (2001). Stem cell self-renewal specified by JAK-STAT activation in response to a support cell cue. *Science* **294**, 2542-2545.
- Lai, Z. C., Fortini, M. E. and Rubin, G. M.** (1991). The embryonic expression patterns of *zfh-1* and *zfh-2*, two *Drosophila* genes encoding novel zinc-finger homeodomain proteins. *Mech Dev* **34**, 123-134.
- Laktionov, P. P., White-Cooper, H., Maksimov, D. A. and Beliakin, S. N.** (2014). [Transcription factor comr acts as a direct activator in the genetic program controlling spermatogenesis in *D. melanogaster*]. *Mol Biol (Mosk)* **48**, 153-165.
- Le Bras, S. and Van Doren, M.** (2006). Development of the male germline stem cell niche in *Drosophila*. *Dev Biol* **294**, 92-103.

- Leatherman, J. L. and Dinardo, S.** (2008). Zfh-1 controls somatic stem cell self-renewal in the *Drosophila* testis and nonautonomously influences germline stem cell self-renewal. *Cell Stem Cell* **3**, 44-54.
- (2010). Germline self-renewal requires cyst stem cells and stat regulates niche adhesion in *Drosophila* testes. *Nat Cell Biol* **12**, 806-811.
- Lee, T. and Luo, L.** (1999). Mosaic analysis with a repressible cell marker for studies of gene function in neuronal morphogenesis. *Neuron* **22**, 451-461.
- Losick, V. P., Morris, L. X., Fox, D. T. and Spradling, A.** (2011). *Drosophila* stem cell niches: a decade of discovery suggests a unified view of stem cell regulation. *Dev Cell* **21**, 159-171.
- Ma, Q., Wawersik, M. and Matunis, E. L.** (2014). The Jak-STAT target Chinmo prevents sex transformation of adult stem cells in the *Drosophila* testis niche. *Dev Cell* **31**, 474-486.
- Marshall, O. J. and Brand, A. H.** (2015). damidseq_pipeline: an automated pipeline for processing DamID sequencing datasets. *Bioinformatics* **31**, 3371-3373.
- Meng, Z., Moroishi, T. and Guan, K. L.** (2016). Mechanisms of Hippo pathway regulation. *Genes Dev* **30**, 1-17.
- Mi, H., Poudel, S., Muruganujan, A., Casagrande, J. T. and Thomas, P. D.** (2016). PANTHER version 10: expanded protein families and functions, and analysis tools. *Nucleic Acids Res* **44**, D336-342.
- Michel, M., Kupinski, A. P., Raabe, I. and Bokel, C.** (2012). Hh signalling is essential for somatic stem cell maintenance in the *Drosophila* testis niche. *Development* **139**, 2663-2669.
- Michel, M., Raabe, I., Kupinski, A. P., Perez-Palencia, R. and Bökel, C.** (2011). Local BMP receptor activation at adherens junctions in the *Drosophila* germline stem cell niche. *Nat Commun* **2**, 415.
- Negre, N., Brown, C. D., Ma, L., Bristow, C. A., Miller, S. W., Wagner, U., Kheradpour, P., Eaton, M. L., Loriaux, P., Sealfon, R., et al.** (2011). A cis-regulatory map of the *Drosophila* genome. *Nature* **471**, 527-531.
- Port, F., Chen, H. M., Lee, T. and Bullock, S. L.** (2014). Optimized CRISPR/Cas tools for efficient germline and somatic genome engineering in *Drosophila*. *Proc Natl Acad Sci U S A* **111**, E2967-2976.
- Postigo, A. A. and Dean, D. C.** (1999). ZEB represses transcription through interaction with the corepressor CtBP. *Proc Natl Acad Sci U S A* **96**, 6683-6688.
- Scadden, D. T.** (2014). Nice neighborhood: emerging concepts of the stem cell niche. *Cell* **157**, 41-50.
- Schindelin, J., Arganda-Carreras, I., Frise, E., Kaynig, V., Longair, M., Pietzsch, T., Preibisch, S., Rueden, C., Saalfeld, S., Schmid, B., et al.** (2012). Fiji: an open-source platform for biological-image analysis. *Nat Methods* **9**, 676-682.
- Singh, S. R., Liu, Y., Zhao, J., Zeng, X. and Hou, S. X.** (2016). The novel tumour suppressor Madm regulates stem cell competition in the *Drosophila* testis. *Nat Commun* **7**, 10473.
- Smedley, D., Haider, S., Ballester, B., Holland, R., London, D., Thorisson, G. and Kasprzyk, A.** (2009). BioMart--biological queries made easy. *BMC Genomics* **10**, 22.

- Southall, T. D., Gold, K. S., Egger, B., Davidson, C. M., Caygill, E. E., Marshall, O. J. and Brand, A. H.** (2013). Cell-type-specific profiling of gene expression and chromatin binding without cell isolation: assaying RNA Pol II occupancy in neural stem cells. *Dev Cell* **26**, 101-112.
- Su, M. T., Fujioka, M., Goto, T. and Bodmer, R.** (1999). The *Drosophila* homeobox genes *zfh-1* and *even-skipped* are required for cardiac-specific differentiation of a *numb*-dependent lineage decision. *Development* **126**, 3241-3251.
- Sun, S., Zhao, S. and Wang, Z.** (2008). Genes of Hippo signaling network act unconventionally in the control of germline proliferation in *Drosophila*. *Dev Dyn* **237**, 270-275.
- Szymczak, A. L., Workman, C. J., Wang, Y., Vignali, K. M., Dilioglou, S., Vanin, E. F. and Vignali, D. A.** (2004). Correction of multi-gene deficiency in vivo using a single 'self-cleaving' 2A peptide-based retroviral vector. *Nat Biotechnol* **22**, 589-594.
- Tapon, N., Harvey, K. F., Bell, D. W., Wahrer, D. C., Schiripo, T. A., Haber, D. and Hariharan, I. K.** (2002). *salvador* Promotes both cell cycle exit and apoptosis in *Drosophila* and is mutated in human cancer cell lines. *Cell* **110**, 467-478.
- Tulina, N. and Matunis, E.** (2001). Control of stem cell self-renewal in *Drosophila* spermatogenesis by JAK-STAT signaling. *Science* **294**, 2546-2549.
- Venken, K. J., Schulze, K. L., Haelterman, N. A., Pan, H., He, Y., Evans-Holm, M., Carlson, J. W., Levis, R. W., Spradling, A. C., Hoskins, R. A., et al.** (2011). MiMIC: a highly versatile transposon insertion resource for engineering *Drosophila melanogaster* genes. *Nat Methods* **8**, 737-743.
- Vogel, M. J., Peric-Hupkes, D. and van Steensel, B.** (2007). Detection of in vivo protein-DNA interactions using DamID in mammalian cells. *Nat Protoc* **2**, 1467-1478.
- Xie, T. and Spradling, A. C.** (2000). A niche maintaining germ line stem cells in the *Drosophila* ovary. *Science* **290**, 328-330.
- Yu, J., Zheng, Y., Dong, J., Klusza, S., Deng, W. M. and Pan, D.** (2010). *Kibra* functions as a tumor suppressor protein that regulates Hippo signaling in conjunction with Merlin and Expanded. *Dev Cell* **18**, 288-299.
- Zhang, L., Ren, F., Zhang, Q., Chen, Y., Wang, B. and Jiang, J.** (2008). The TEAD/TEF family of transcription factor Scalloped mediates Hippo signaling in organ size control. *Dev Cell* **14**, 377-387.
- Zhu, L. J., Gazin, C., Lawson, N. D., Pages, H., Lin, S. M., Lapointe, D. S. and Green, M. R.** (2010). ChIPpeakAnno: a Bioconductor package to annotate ChIP-seq and ChIP-chip data. *BMC Bioinformatics* **11**, 237.

Figures

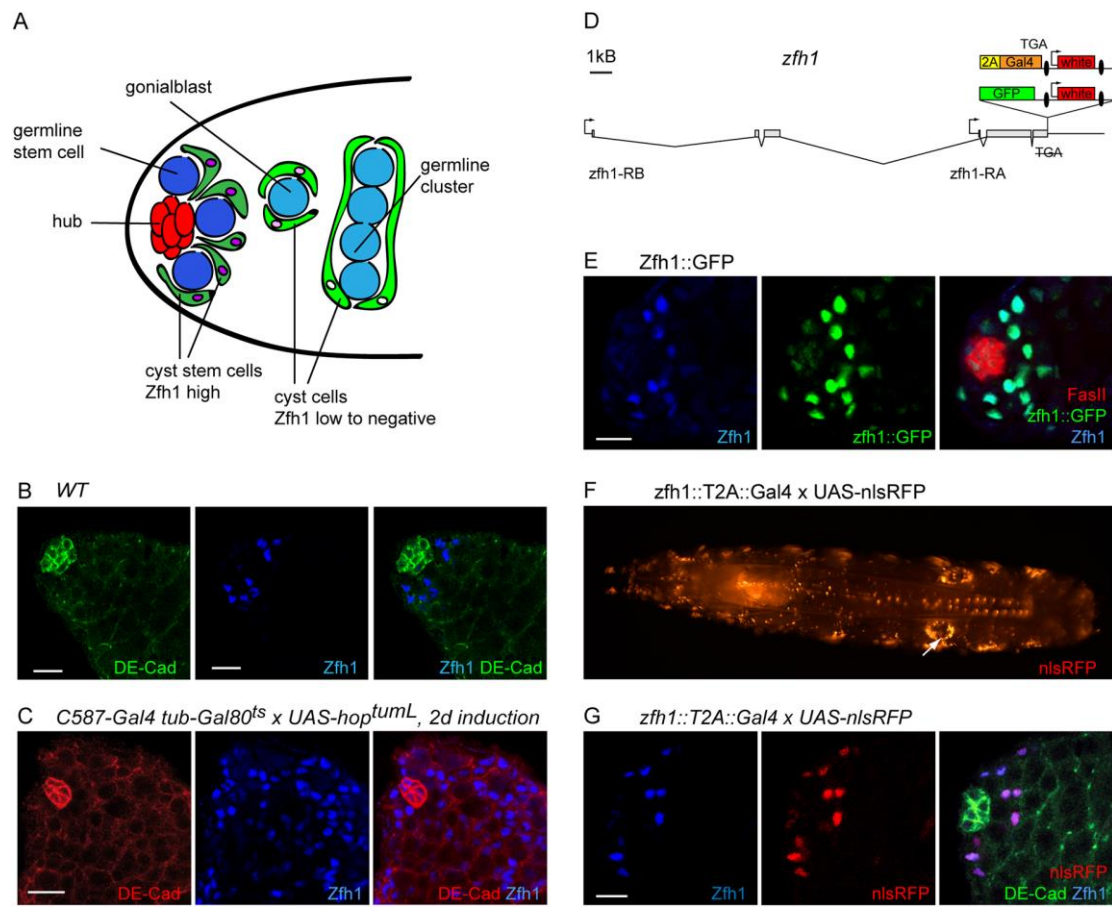


Figure 1 - Endogenous Zfh1 expression and Crispr/Cas9 generated reagents

A Schematic representation of the stem cell niche of the *Drosophila* testis tip. Zfh1 (magenta) marks the nuclei of the cyst stem cells (CySCs) and, at lower levels, their immediate progeny.

B CySCs are recognized by their Zfh1 positive nuclei (blue) and their position adjacent to the hub (identified by strong DE-Cad expression, green).

C Zfh1 positive cells (blue) expand following a 2d pulse of the constitutively active Jak kinase Hop^{tumL}. Hub and CyC outlines marked by DE-Cad (red).

D Schematic representation of the Zfh1 locus and C-terminal GFP and T2A-Gal4 fusions. Small ellipses indicate loxP sites flanking the white⁺ transgenesis marker.

E Zfh1::GFP (green) colocalizes with Zfh1 immunostaining (blue) in the vicinity of the hub (FasIII, red).

F,G nlsRFP expression under control of *zfh1::T2A::Gal4*. **F** In the larva, RFP is expressed in multiple tissues including the testis (arrow). **G** In the adult testis nlsRFP (red) coincides with Zfh1 protein (blue) labelling the CySCs abutting the hub (DE-Cad, green).

Scale bars 10 μ m.

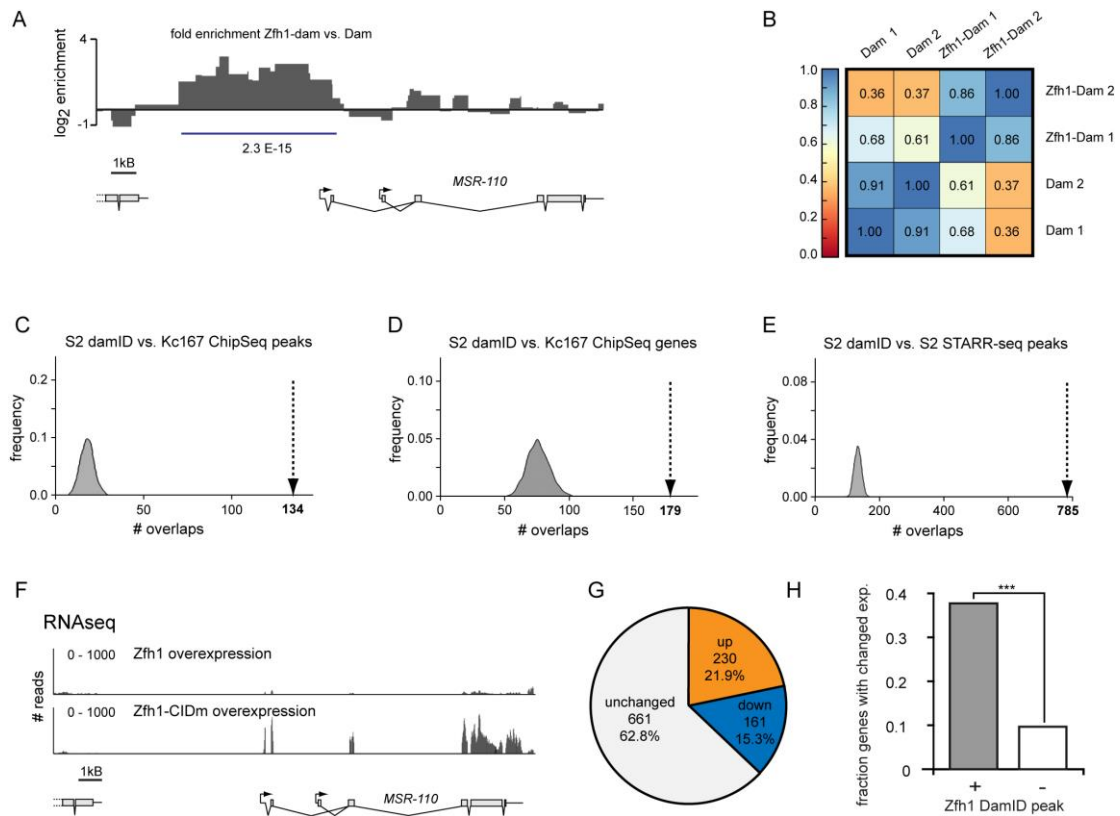


Figure 2 - Zfh1 DamID in S2 cells

A NGS reads from a Zfh1-Dam sample are enriched relative to a Dam only control (bottom panel) near the MSR-110 distal transcription start (log₂ of ratio plotted vs. genome position; peak as called by damid_seq, blue line; FDR indicated).

B Pearson's correlation between S2 cell Zfh1-Dam and Dam control samples, two biological replicates.

C-E Overlap of Zfh1 DamID peaks in S2 cells or their respective, associated genes with data sets from ChipSeq and STARR-Seq experiments. Distribution of overlaps from 1000 simulated resamplings of the Zfh1 peaks plotted against frequency; dashed arrows indicate experimentally observed values. **C** Zfh1 DamID peaks in S2 cells show significant overlap with Zfh1 ChIP peaks in Kc167 cells ($p < 0.001$, permutation test). **D** Genes associated with Zfh1 DamID peaks in S2 cells and Zfh1 ChIP peaks in Kc167 cells show significant overlap ($p < 0.001$, χ^2 -test). **E** Zfh1 DamID peaks in S2 cells overlap with enhancer regions identified by STARR-seq ($p < 0.001$, permutation test).

F-H Transcriptional differences between S2 cells overexpressing either WT Zfh1 or a Zfh1 construct unable to bind CtBP (zfh1-CIDm). **F** Number of RNAseq reads plotted against genomic position reveals transcriptional derepression of the *MSR-110* gene in response to Zfh1-CIDm. **G** Response to zfh1-CIDm overexpression relative to Zfh1 control by genes associated with a Zfh1 DamID peak. **H** Genes associated with a Zfh1 DamID peak are significantly more likely than other genes to exhibit differences in transcription levels between Zfh1 and Zfh1-CIDm samples (***, $p < 0.001$, χ^2 -test).

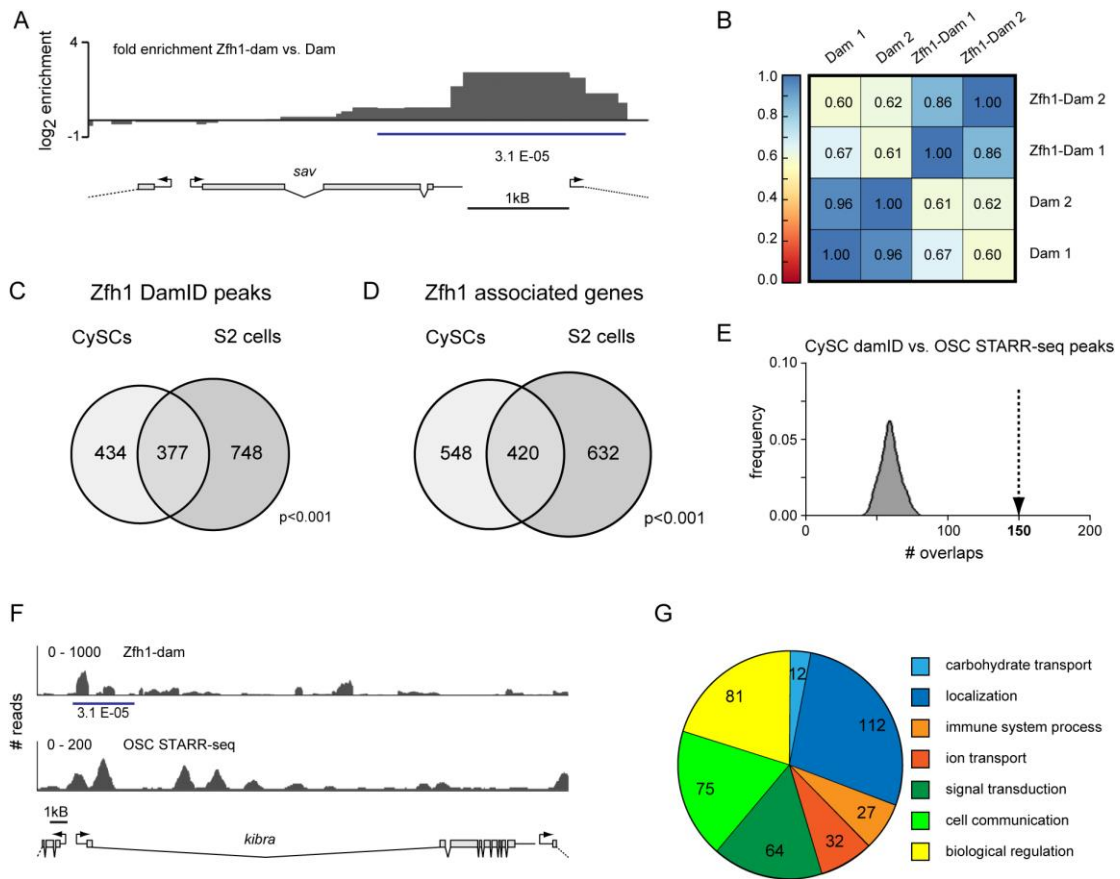


Figure 3 - *In vivo* Zfh1 DamID in CySC cells

A Zfh1 DamID reads are enriched near the 3'-UTR and downstream intergenic region of the *sav* locus (extent of DamID peak, blue line; FDR indicated).

B Pearson's correlation between CySC *in vivo* DamID samples, two biological replicates.

C,D 46% of CySC DamID peaks **C** and 43% of the associated genes **D** are also recovered in S2 cells, significantly more than expected by chance (C, $p < 0.001$, permutation test; D, $p < 0.001$, χ^2 -test).

E CySC Zfh1 DamID peaks overlap with enhancer regions in ovarian somatic cell ($p < 0.001$, permutation test)

F Comparison of Zfh1 DamID peaks in CySCs and STARR-seq peaks in cultured ovarian stem cells for the *kibra* locus

G GO-slim terms enriched among Zfh1 associated genes.

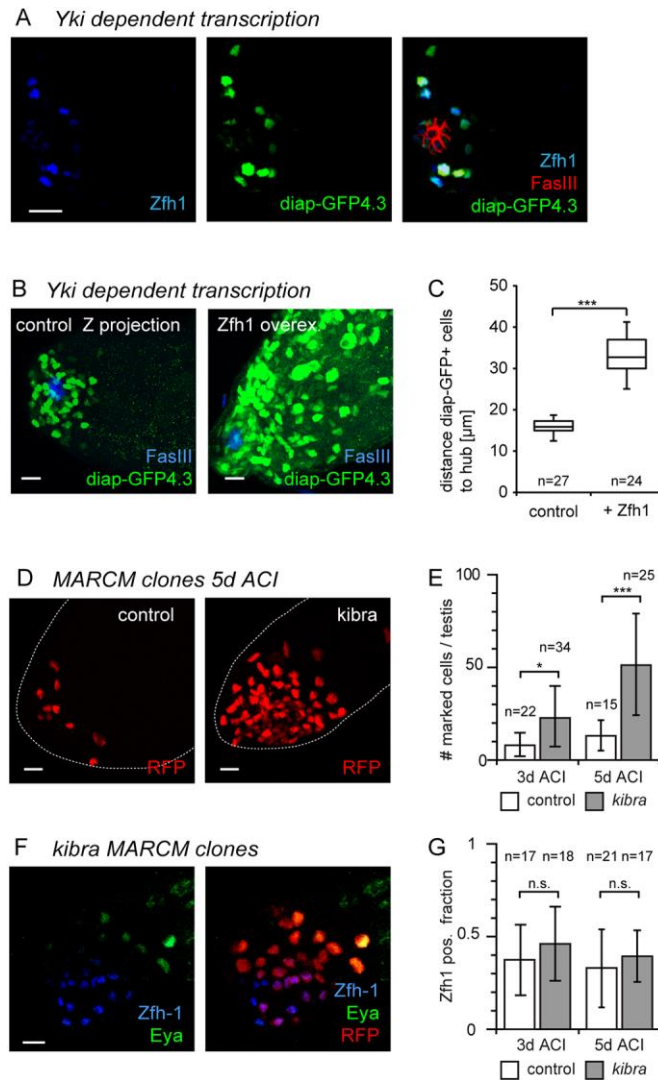


Figure 4 - The Hippo pathway controls CySC proliferation

A Activity of a transcriptional reporter (green) driving GFP expression from a Yki dependent fragment of the diap1 promoter (diap-GFP4.3) is restricted to Zfh1 positive CySCs (blue). Hub marked by FasIII (red).

B Zfh1 overexpression under *tj*-Gal4 control for 8d expands the population of cells with active Yki to regions further from the hub (FasIII, blue).

C Quantification of the average distance of diap-GFP4.3 positive cells to the hub in controls vs. testes overexpressing Zfh1 under *tj*-Gal4 control for 8d (n, number of testes). Box indicates first and third quartile; horizontal line, median; square, mean; whiskers, data range up to 1.5x interquartile distance.

D Homozygous *kibra* mutant MARCM clones (RFP, red) overproliferate relative to control clones.

E Quantification of homozygous *kibra* or control cells per testis (n, number of testes)

F) *kibra* mutant cells (RFP, red) within the same testis overlap both with the stem cell marker *Zfh1* (blue) and the differentiation marker *Eya* (green).

G *kibra* and control clones do not differ in the fraction of *Zfh1* positive clonal cells.

Bar graphs, mean \pm SD. *, $p < 0.05$ ***, $p < 0.01$ (t-test), n.s., not significant. Scale bars 10 μ m.

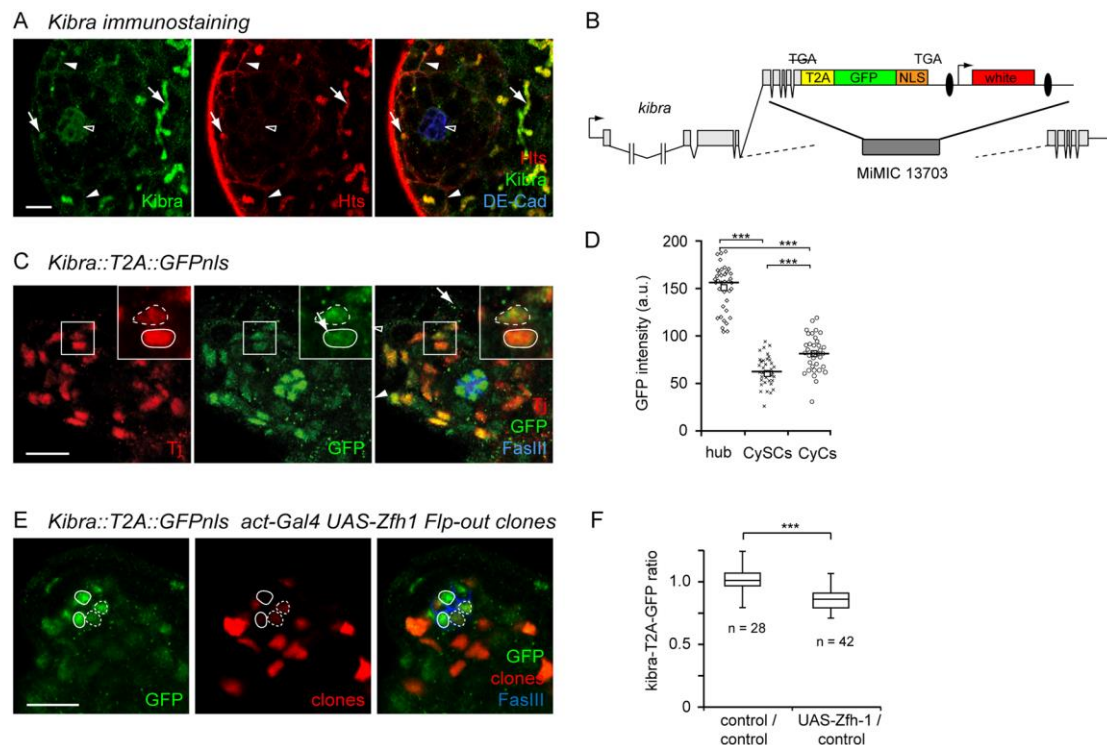


Figure 5 - Kibra expression in the testis

A *Kibra* immunostaining (green) is detectable in the somatic hub cells (DE-Cad, blue, hollow arrowhead) as well in punctate structures corresponding to spectrosomes and fusomes of the germline (Hts, red, arrows). Diffuse cortical *Kibra* staining around cell outlines (solid arrowheads) cannot be assigned unambiguously to either lineage.

B *kibra*-T2A-GFPnls construct inserted into a MiMIC landing site preceding exon 5. Ellipses, loxP sites.

C-F GFP immunostaining in the *Kibra*-T2A-GFPnls reporter line.

C Nuclear GFP is visible both in the germline (large, diffusely stained nuclei) and the somatic lineage, with pronounced staining in the hub (FasIII, blue). Note reduced signal in CySC nuclei identified as Tj-positive (red) nuclei abutting the hub (solid outline in inset) relative to their CyC neighbours (dashed outline).

D Quantification of GFP intensities in **C** for the different cell types, n=13 testes. Solid line, median; square, mean; ***, p<0.01 (ANOVA).

E *Zfh1* overexpression in RFP marked Flp-out clones (red, dashed outline) in the hub (FasIII, blue) decreases nuclear GFP levels (green) relative to sibling cells (solid outline).

F Ratio of GFP immunofluorescence between Zfh1 expressing and adjacent non-expressing nuclei or between controls. Box indicates first and third quartile and median. Whiskers indicate data range up to 1.5x interquartile distance. ***, $p < 0.01$ (t-test).

Scale bars 10 μ m.

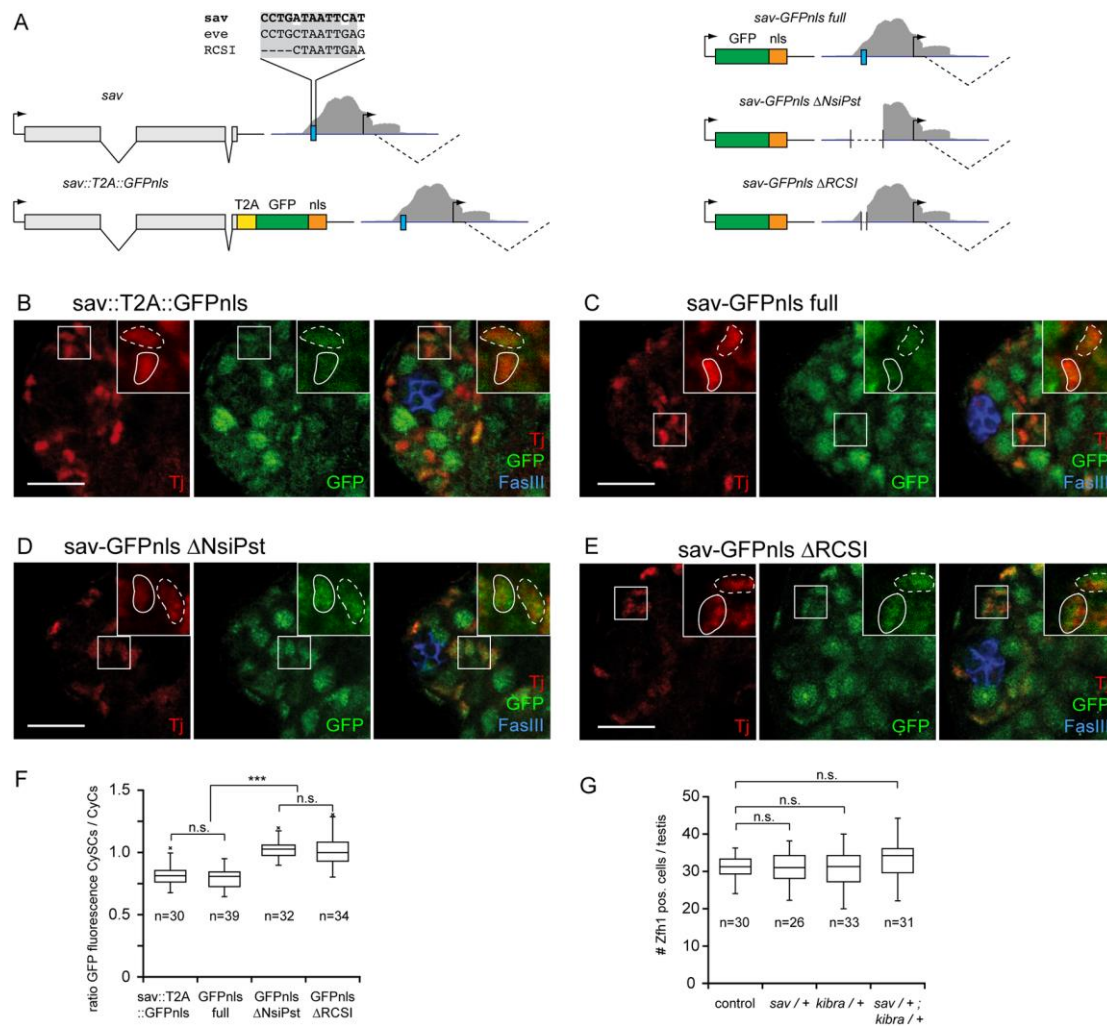


Figure 6 - Sav in the adult testis

A Organization of the *sav* locus, the *sav*-T2A-GFPnls construct, and the *sav*::GFPnls transcriptional reporters. Blue line, extent of Zfh1 DamID peak (gray shading). Blue box, RCSI-like putative Zfh1 binding site. Sequences from *sav*, the *eve* Zfh1 binding site, and the original RCSI sequence are indicated.

B-E GFP immunofluorescence from the *sav* reporter constructs. Note GFP signal (green) in the large germline nuclei and smaller somatic nuclei (marked by Tj, red); hub marked by FasIII (blue).

B,C In the *sav*-T2A-GFPnls fusion construct (**B**) and the *sav*::GFP_full transcriptional reporter (**C**) the GFP signals in CySC nuclei (identified by proximity to hub, solid outline) are reduced relative to the adjacent CyC nuclei (dashed outlines).

D, E In *sav::GFPnls_ΔNsiPst* (**D**) and *sav::GFPnls_ΔRCSI* (**E**) transgenic flies the difference in GFP intensity between CySC and CyC nuclei vanishes.

F Quantification of the GFP intensity ratios between pairs of adjacent CySC and CyC nuclei for **B-E**.

G Quantification of *Zfh1* positive cells for controls and *sav* and *kibra* single and double heterozygous males (n, number of testes).

Scale bars 10μm. Box indicates first and third quartile and median. Whiskers indicate data range up to 1.5x interquartile distance. Outliers marked individually; ***, p<0.01 (ANOVA); n.s., not significant.

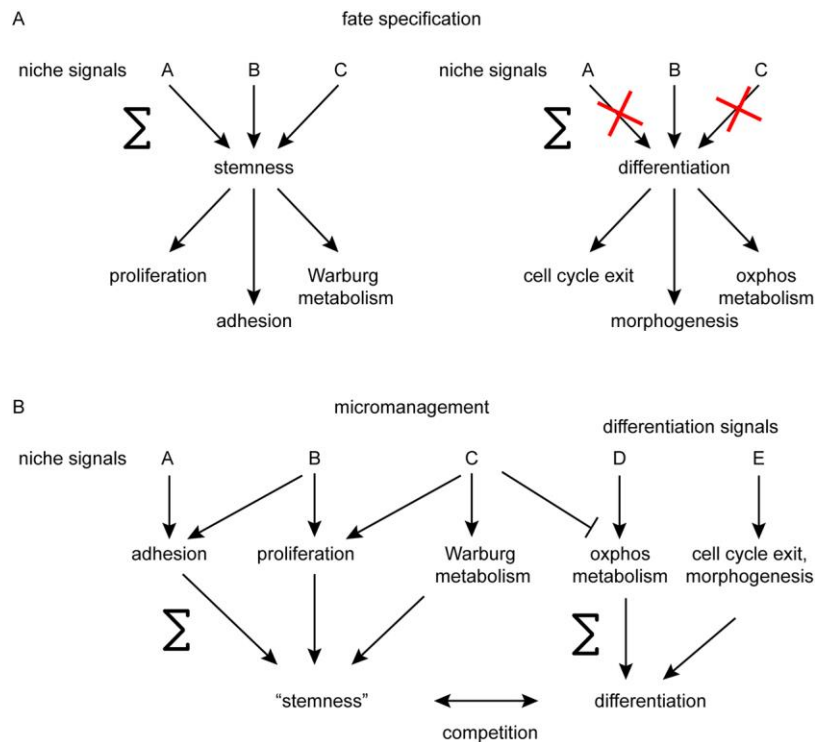


Figure 7 - Models of stemness and niche function

A According to the standard model, multiple niche signals are integrated into a decision to adopt stem cell fate. Differentiation is the default response when some of these signals are absent. Explaining why increasing one particular niche signal can impinge on only one or few aspects of stem cell behaviour, thus uncoupling these traits, is not straightforward.

B Under the proposed micromanagement model, niche signals continuously control genetically separable subsets of stem cell behavioural output. Stemness becomes a compound phenotype rather than a binary cell fate. Differentiation is similarly specified by additional signals that include cues from the intense cell competition in the niche.

Supplementary Information

Table S1: Zfh1 DamID peaks and associated genes from S2 cells

[Click here to Download Table S1](#)

Table S2: Transcripts with altered expression levels in S2 cells overexpressing Zfh1-CIDm vs. Zfh1

[Click here to Download Table S2](#)

Table S3: Zfh1 DamID peaks and associated genes from CySCs
Supplementary figures S1 - S5

[Click here to Download Table S3](#)

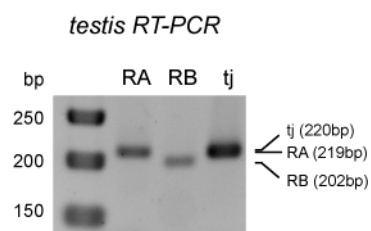


Figure S1 - Expression of Zfh1 isoforms

RT-PCR on adult testis mRNA extracts reveals expression of both Zfh1-RA and -RB isoforms. tj, expression control.

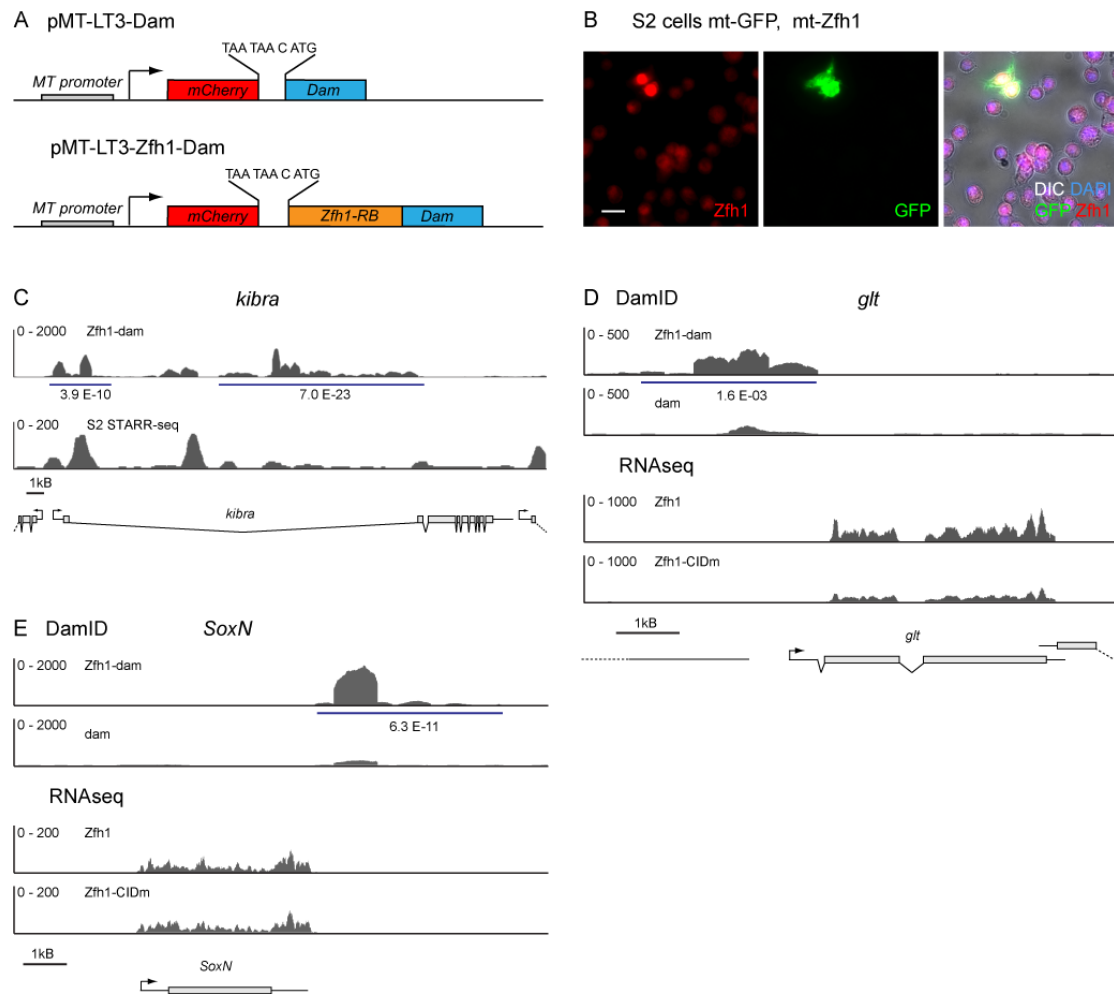


Figure S2 - Zfh1 in S2 cells

A Schematic representation of the DamID vectors used for stable transfection. Levels of Dam and the Zfh1-Dam fusion protein are minimized by the presence of an mCherry leader ORF termed LT3 followed by two stop codons and a frame shift that limits expression to rare transcriptional reinitiation events.

B S2 cells transiently cotransfected with plasmids expressing either Zfh1 or GFP under control of the metallothionein (mt) promoter. Following a 24h induction, strong Zfh1 immunostaining (red) is visible in GFP positive (green) nuclei, while a weaker, endogenous Zfh1 signal can also be seen in the nontransfected cells. Nuclei marked by DAPI (blue), cell outlines by DIC (grayscale).

C One of the two DamID peaks identified at the *kibra* locus that is localized near the transcriptional start site overlaps with a transcriptional activator region identified by STARR-seq.

D The *glt* gene is associated with a single, 5' localized Zfh1 DamID peak and exhibits reduced transcription following overexpression of the Zfh1-CIDm construct unable to bind the CtBP transcriptional corepressor.

E The *SoxN* gene is associated with a single, 3' localized Zfh1 DamID peak but does not exhibit any change in transcription following Zfh1-CIDm overexpression.

Peaks called by damid_seq marked by blue line; FDR indicated.

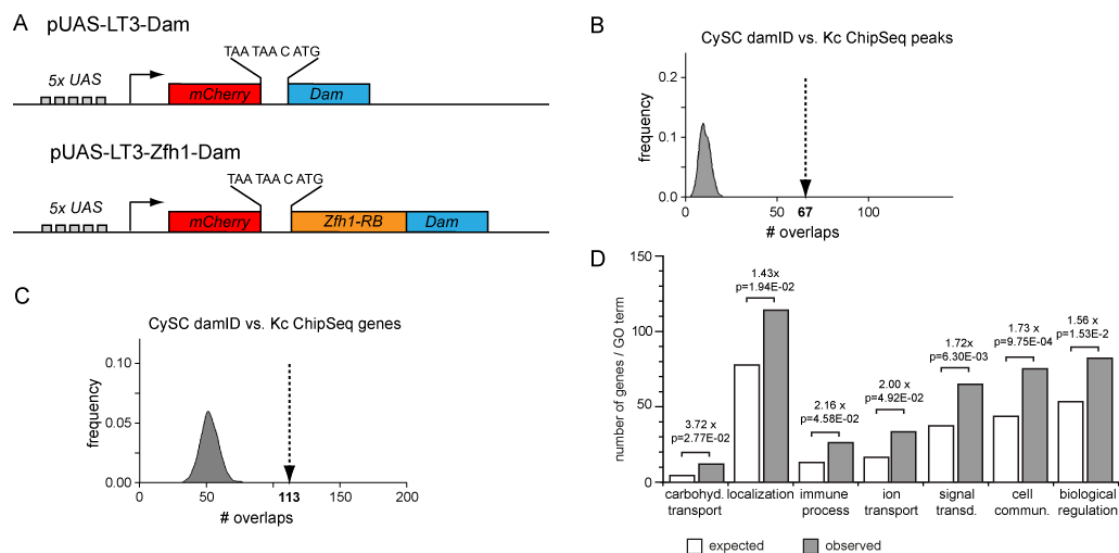


Figure S3 - Zfh1 DamID in S2 cells

A Schematic representation of the DamID vectors used for UAS/Gal4 driven expression in the CySCs. Levels of Dam and the Zfh1-Dam fusion protein are again minimized by the presence of an mCherry leader ORF termed LT3 followed by two stop codons and a frame shift.

B Zfh1 DamID peaks in CySCs significantly colocalize with Zfh1 ChIP peaks in Kc167 cells ($p<0.001$, permutation test). Distribution of overlaps from 1000 resamplings plotted against frequency; dashed arrow indicates observed overlap.

C Same as **B** for the respective associated genes (DamID peak falling within transcript region ± 1 kb, $p<0.001$, χ^2 -test).

D GO-slim terms overrepresented for genes associated with at least one Zfh1 DamID peak in CySCs. Expected and observed numbers of genes, enrichment factor, and p-value given for terms exhibiting significant overrepresentation.

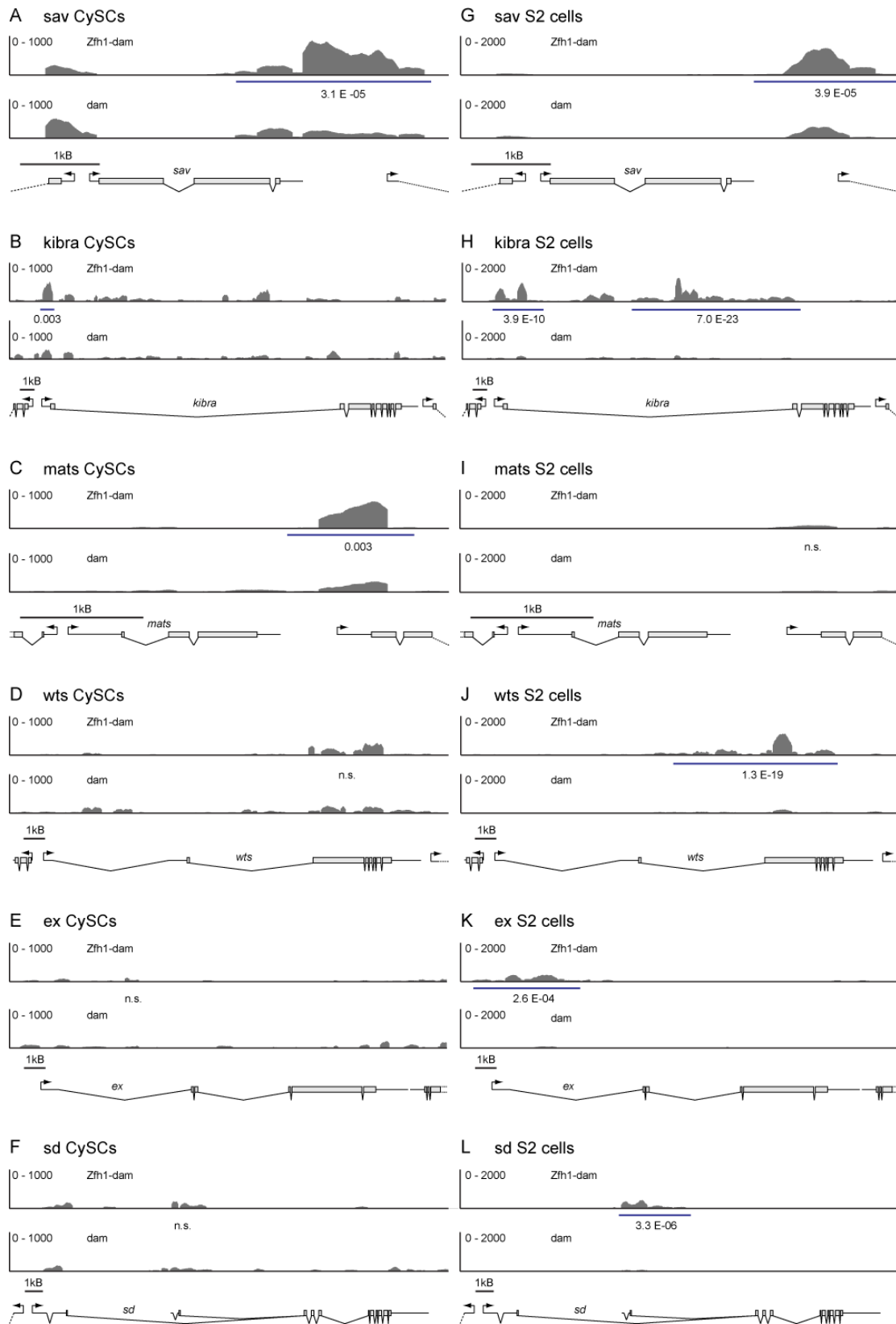


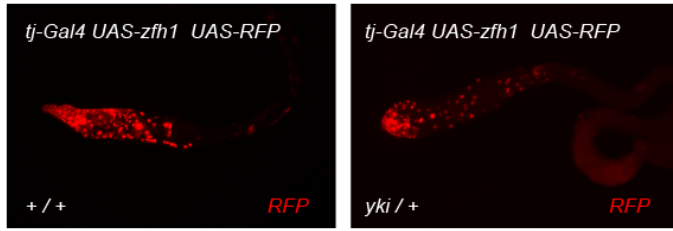
Figure S4 - Zfh1 DamID peaks near Hippo pathway components

A-E NGS reads from Zfh1-Dam (top panel) and Dam only control samples (bottom) panels for selected components of the Hippo pathway reveals Zfh1 binding peaks in CySCs.

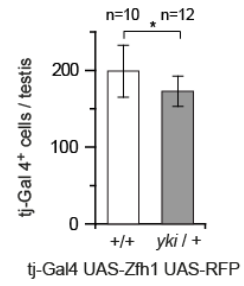
G-K Same for S2 cells.

DamID peaks as called by damid_seq, blue line; FDR indicated.

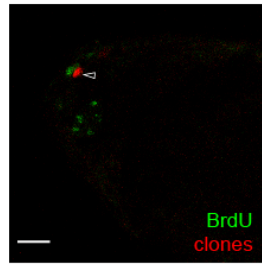
A Yki dosage sensitivity of Zfh1 driven proliferation



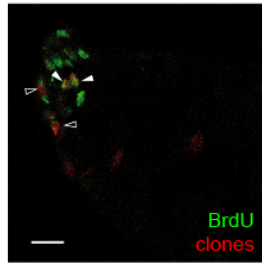
B



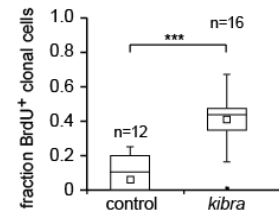
C control



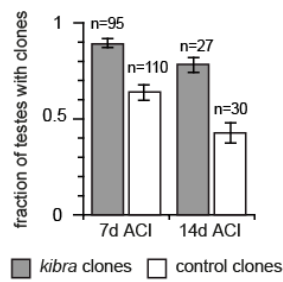
kibra MARCM clones



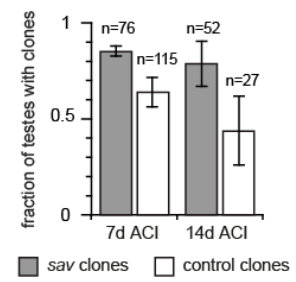
D



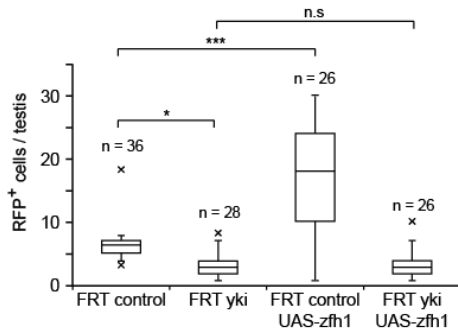
E



F



G



H

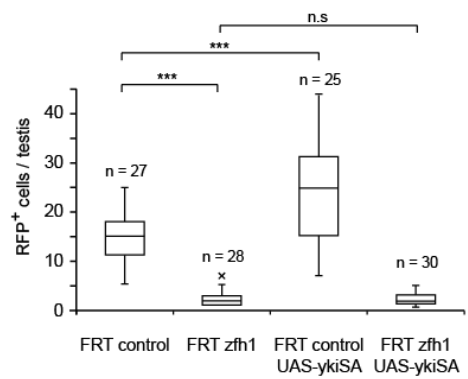


Figure S5 - Hippo signalling and CySC maintenance and proliferation

A Overexpression of UAS-Zfh1 under Tj-Gal4 control for five days causes expansion of somatic cells as visualized by co-overexpression of UAS-nlsRFP.

B Quantification of the RFP positive nuclei reveals a 14% reduction in number when one copy of *yki* is removed.

C Following an 8h pulse of BrdU feeding, *kibra* MARCM clones (RFP, red) contained a larger fraction of BrdU (green) positive cells than corresponding, neutral control clones.

D Quantification of the fraction of BrdU positive cells relative to the total number of cells per clone.

E Compared with control clones, which are gradually lost over time, homozygous *kibra* clones are retained in a larger fraction of testes one or two weeks ACI.

F Same as **E** for homozygous *sav* and control clones.

G,H Epistasis analysis for Yki and Zfh1. **G**, Loss of Yki reduces clone size (as reflected by the number of RFP positive cells per testis). This cannot be rescued by clonal overexpression of Zfh1, even though this is in control clones sufficient to increase the number of marked cells. **H**, Overexpression of activated, nonphosphorylatable Yki can conversely not rescue the loss of RFP positive cells homozygous mutant for *zfh1* even though it is sufficient to expand control clones.

Scale bars, 10 μ m. **B,E,F**: Columns indicate mean, error bars standard deviation **D,G,H**: Box indicates first and third quartile and median. Whiskers indicate data range up to 1.5x interquartile distance. Outliers marked individually. *, p<0.05; ***, p<0.001 (**B,D**: t-test, **G,H**: Anova); n, number of testes.